EXTREME ULTRAVIOLET ASTRONOMY

MARTIN A. BARSTOW
University of Leicester, UK

JAY B. HOLBERG
University of Arizona, Tucson, USA

CAMBRIDGE
UNIVERSITY PRESS

PUBLISHED BY THE PRESS SYNDICATE OF THE UNIVERSITY OF CAMBRIDGE
The Pitt Building, Trumpington Street, Cambridge, United Kingdom

CAMBRIDGE UNIVERSITY PRESS
The Edinburgh Building, Cambridge CB2 2RU, UK
40 West 20th Street, New York, NY 10011-4211, USA
477 Williamstown Road, Port Melbourne, VIC 3207, Australia
Ruiz de Alarcón 13, 28014 Madrid, Spain
Dock House, The Waterfront, Cape Town 8001, South Africa

http://www.cambridge.org

First published 2003

Printed in the United Kingdom at the University Press, Cambridge

Typefaces Times Roman 10/12.5 pt and Gill Sans *System* LaTeX 2$_\varepsilon$ [TB]

A catalogue record for this book is available from the British Library

Library of Congress Cataloguing in Publication data

Barstow, Martin A. (Martin Adrian), 1958–
Extreme ultraviolet astronomy : EUV astronomy / Martin A. Barstow, Jay B. Holberg.
p. cm.
Includes bibliographical references and index.
ISBN 0 521 58058 7
1. Ultraviolet astronomy. I. Holberg, J. B. II. Title.
QB474 .B37 2002 522′.68–dc21 2002073705

ISBN 0 521 58058 7 hardback

Contents

1

Introduction to the Extreme Ultraviolet: first source discoveries

1.1 Astrophysical significance of the EUV

The Extreme Ultraviolet (EUV) nominally spans the wavelength range from 100 to 1000 Å, although for practical purposes the edges are often somewhat indistinct as instrument bandpasses extend shortward into the soft X-ray or longward into the far ultraviolet (far UV). Like X-ray emission, the production of EUV photons is primarily associated with the existence of hot gas in the Universe. Indeed, X-ray astronomy has long been established as a primary tool for studying a diverse range of astronomical objects from stars through to clusters of galaxies. An important question is what information can EUV observations provide that cannot be obtained from other wavebands? In broad terms, studying photons with energies between ultraviolet (UV) and X-ray ranges means examining gas with intermediate temperature. However, the situation is really more complex. For example, EUV studies of hot thin plasma in stars deal mainly with temperatures between a few times 10^5 and a few times 10^6 K, while hot blackbody-like objects such as white dwarfs are bright EUV sources at temperatures a factor of 10 below these. Perhaps the most significant contribution EUV observations can make to astrophysics in general is by providing access to the most important spectroscopic features of helium – the He I and He II ground state continua together with the He I and He II resonance lines. These are the best diagnostics of helium, the second most cosmically abundant element, with the line series limits at 504 Å and 228 Å for He I and He II respectively.

Sources of EUV radiation can be divided into two main categories: those where the emission arises from recombination of ions and electrons in a hot, optically thin plasma, giving rise to emission line spectra (figure 1.1); and objects that are seen by thermal emission from an optically thick medium, resulting in a strong continuum spectrum but which may contain features arising from transitions between different energy levels or ionisation stages of several elements (figure 1.2).

Examples of the former category are single stars and binary systems containing active coronae, hot O and B stars with winds, supernova remnants and galaxy clusters. Hot white dwarfs, central stars of planetary nebulae (CSPN) and neutron stars are all possible continuum sources. Cataclysmic binaries, where material is being transferred from a normal main sequence star (usually a red dwarf) onto a white dwarf, may well contain regions of both optically thin and optically thick plasma. In O and B stars the EUV emission will be dominated by emission from the shocked wind plasma only at short wavelengths while at longer wavelengths, below the Lyman limit, the continuum flux will be the most important. Apart from studying directly the EUV emission from astronomical objects, these same sources can potentially be used as probes of the interstellar medium. The absorbing

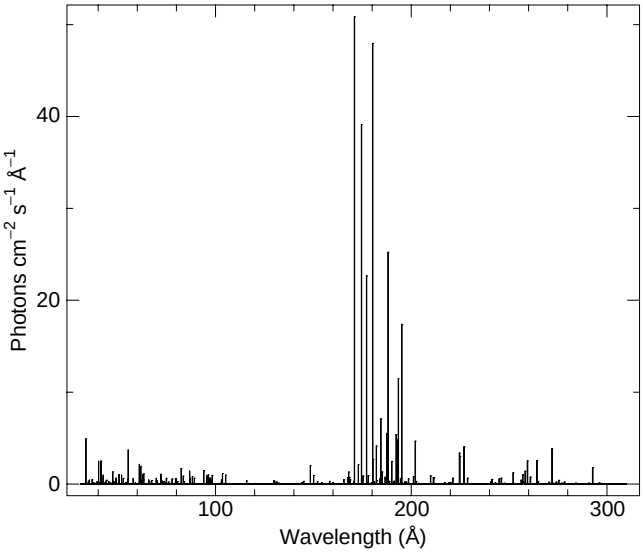

Fig. 1.1. An example of an emission line spectrum in the EUV, arising from a 10^6 K optically thin plasma. The strongest group of lines in the region 170 to 200 Å are mainly Fe transitions (Fe IX to Fe XII).

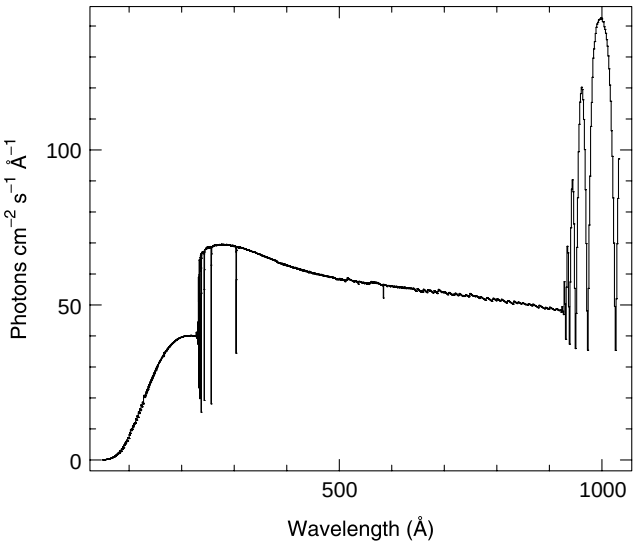

Fig. 1.2. Continuum spectrum in the EUV, formed in this example in the hot photosphere of a 50 000 K white dwarf. The absorption features near 1000 Å are the H I Lyman series and those near 228 Å correspond to the Lyman series of He II, with an assumed abundance (by number) $\mathrm{He/H} = 1 \times 10^{-5}$.

effect of the interstellar medium can modify the flux received at the Earth allowing, if the properties of the radiating source are well understood, its structure and density to be studied.

EUV observations can be used to study a wide variety of astronomical environments and physical processes. The aim of this book is to present the scientific discoveries arising from cosmic EUV astronomy, discussing some of the underlying physics to illustrate the insights that can be gained from this work. Since this field has only recently become a fully-fledged branch of astronomy, we present the information in a historical context dealing with the development of both observational and instrumental areas of the subject.

1.2 The 'unobservable ultraviolet'

Until the early 1970s, the conventional view was held that EUV astronomy was not a practical proposition. Since most elements have outer electron binding energies in the range 10–100 eV, photons in the corresponding energy range will be strongly absorbed in any photon–atom interaction when

$$\chi_i < hc/\lambda \tag{1.1}$$

where λ is the photon wavelength, χ_i is the ionization potential and c is the speed of light.

When $10 < \chi_i < 100$ eV, λ lies in the range 100–1000 Å, i.e. within the EUV band. As a result, the Earth's atmosphere is opaque to EUV radiation due to photoabsorption by N_2, O_2 and O. The $1/e$ absorption depth of the atmosphere is $\approx$130 km at 100 Å. Hence, ground-based EUV astronomy is inconceivable. As in X-ray and far-UV astronomy, this problem can be overcome by placing instrumentation above the atmosphere. However, a more serious problem is posed by absorption of interstellar gas which can potentially make the interstellar medium (ISM) opaque to EUV radiation over interstellar distances (Aller 1959). For example, the mean free path (τ, cm) of a photon in the ISM, where hydrogen is the most abundant element, can be estimated from the known neutral hydrogen density ($n_{\rm H}$, cm^{-3}) and hydrogen absorption cross-section (σ, cm^2), where

$$\tau = 1/(n_{\rm H}\,\sigma) \tag{1.2}$$

In an influential paper, Aller (1959) argued that, based on the then knowledge of the distribution and density of hydrogen in the galaxy, the ISM would be completely opaque at wavelengths between the X-ray band and Lyman limit at 912 Å and EUV observations impossible. This calculation assumes an interstellar value of 1 atom cm^{-3} for $n_{\rm H}$, inferred from 21 cm radiowave surveys. For a neutral hydrogen cross-section of $\approx 10^{-18}$ cm^2, averaged over the entire EUV range, the estimated mean free path (eqn (1.2)) is a mere 10^{18} cm (0.4 parsec) – well below the distance to any astronomical objects other than those in the solar system. Even taking the most optimistic value of the absorbing cross-section (3×10^{-20} cm^2 at 100 Å) gives a viewing distance of only 10 pc. Aller's basic conclusions, self-evident from the knowledge available in 1959, remained unchallenged for more than a decade consigning this region of the electromagnetic spectrum to the 'unobservable ultraviolet' (Harwit 1981).

In contrast to Aller's first, relatively crude estimate of the absorbing effect of the ISM on EUV radiation, Cruddace *et al.* (1974) calculated the interstellar absorption cross-section over

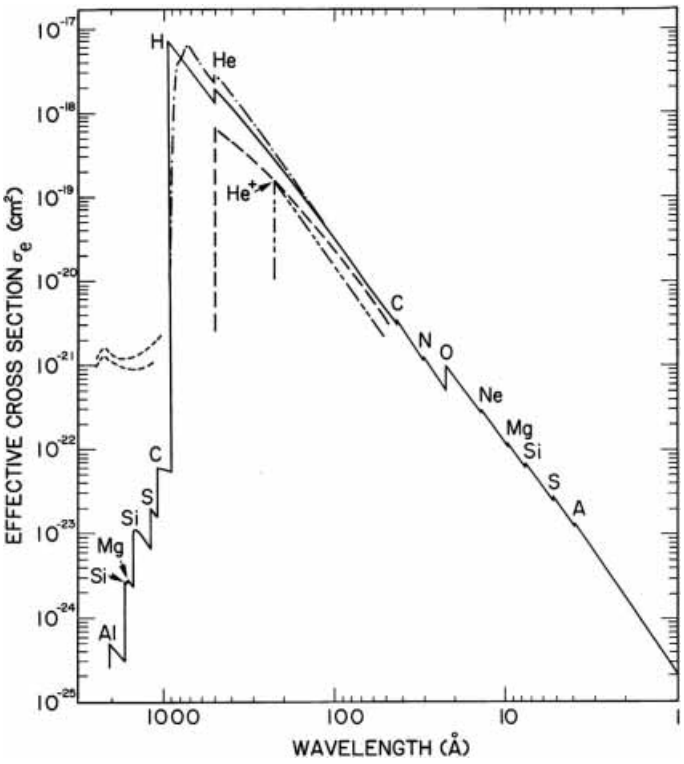

Fig. 1.3. Effective cross-section of the interstellar medium. —— gaseous component with normal composition and temperature; –·– hydrogen, molecular form; — — H II region about a B star; — – – — H II region about an O star; - - - - dust (from Cruddace *et al*. 1974).

the wavelength range 1 to 2000 Å (figure 1.3) and then determined the percentage absorption as a function of wavelength and of n_{H}. These calculations, expressed in figure 1.4 as the distance for 90% attenutation of the radiation, coupled with increasing indirect evidence for lower values of the value of n_{H} along at least some lines-of-sight indicated significant transparency in the EUV window and demonstrated the possibility of being able to 'see' EUV sources out to distances of a few hundred parsecs, at the shorter (100–500 Å) wavelengths. Figure 1.4 conveniently expresses a fundamental observational fact of EUV astronomy – for a given column of interstellar gas the distances at which sources can be detected rapidly shrinks as wavelengths increase. A direct consequence of this is that, in general, the number of sources that can be detected diminishes rapidly at longer wavelengths.

Radio measurements of interstellar hydrogen densities are really measuring the total amount of material along the line-of-sight, over distances of several kiloparsecs. Hence, the estimated volume densities are just averages within these long columns and may not be representative of values for the local ISM (LISM), within the distances of a few hundred parsecs critical for EUV astronomy. Furthermore, at least in the 1950s and 1960s, such measurements were carried out with beams several degrees in angular extent and were unable to detect any possible variations in line-of-sight absorption on scales smaller than this. In the early 1970s far-UV satellite experiments provided the first sensitive localised measurements

Table 1.1. *Neutral hydrogen densities* N_H *along the lines-of-sight to bright stars observed in the far-UV.*

Object	Distance (pc)	$n_{\rm H}$ (cm^{-3})	$N_{\rm H}$ (cm^{-2})	Reference
α Leo	22	0.02	1.4×10^{18}	Rogerson *et al*. 1973
α Eri	24	0.07	5.1×10^{18}	Rogerson *et al*. 1973
α Gru	28	1.16	1.0×10^{20}	Spitzer *et al*. 1973
δ Per	83	0.59	1.5×10^{20}	Spitzer *et al*. 1973
β Cen	90	0.11	3.0×10^{19}	Savage and Jenkins 1972

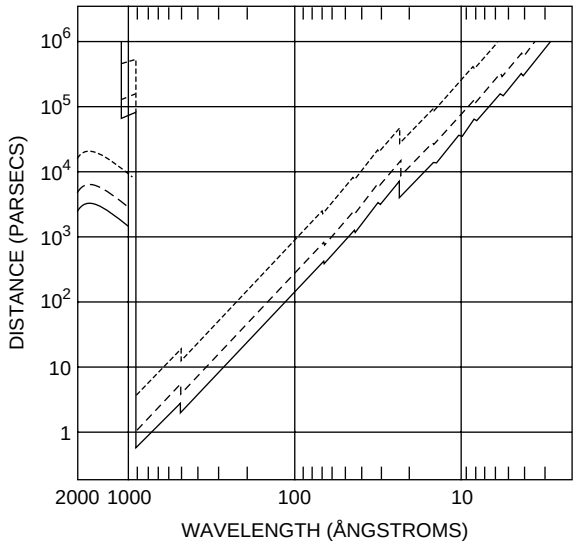

Fig. 1.4. Distance at which attenuation of the incident radiation reaches 90%, as a function of wavelength. An unionised interstellar medium of normal composition is assumed. —— $n_{\rm H} = 0.2\,{\rm cm}^{-3}$; — — $n_{\rm H} = 0.1\,{\rm cm}^{-3}$; – – – $n_{\rm H} = 0.03\,{\rm cm}^{-3}$ (from Cruddace *et al*. 1974).

of $n_{\rm H}$ over much shorter path lengths and narrower angular scales by using the absorption profiles of Lyman α (1216 Å) and Lyman β (1026 Å) in the spectra of bright, unreddened stars (i.e. without the presence of dust along the line-of-sight). Results from studies with Mariner 9 (e.g. Bohlin 1973), OAO–2 (e.g. Savage and Jenkins 1972) and Copernicus (e.g. Rogerson *et al*. 1973; Spitzer *et al*. 1973) showed that the ISM is far from uniformly distributed as had been supposed previously and that 'local' values of $n_{\rm H}$ could be very much lower than 1 atom cm^{-3}. Table 1.1 summarises several of these measurements, showing volume densities ranging from 0.02 to 1.16 atom cm^{-3}.

1.3 Early detectors for the EUV

To observe at wavelengths in the EUV, astronomers in the 1960s and 1970s needed new detector technology. Solar EUV astronomers used specially developed EUV/X-ray sensitive films for the Skylab telescopes and spectrographs. Although such films provided high spatial resolution, they had a number of insurmountable problems for cosmic EUV observations.

First and foremost, the film required returning to Earth for developing, thereby excluding use on unmanned, long-lifetime observatories. Also, such films were not particularly sensitive, and required exceptionally stable pointing (or very short exposures) to be of practical use on spacecraft.

Thus, to make progress in space-based EUV astronomy, sensitive, photon-counting detectors were needed. Two approaches were natural developments from shorter (X-ray) and longer (UV) wavelengths: proportional counters and photomultipliers.

1.3.1 Proportional counters

The proportional counter is based on the familiar *Geiger counter*, a device that gives an audible 'click' and/or deflection of a meter on detection of a radioactive decay product. The rate of clicking depends on the level of radioactivity, i.e. the number of decay products passing through the counter in each second. Such counters consist of a sealed metallic tube containing a gas such as xenon. The tube usually has a thinner area, or window, through which some less-penetrating radiation can pass. Along the central axis of the tube, a thin, very uniform wire is kept at a high voltage (typically 1 kV or more). When a gamma ray ($E > 50$–100 keV or $\lambda < 0.1$ Å) penetrates the gas volume in the Geiger counter, it may ionise a gas atom. The likelihood of this depends upon the gas pressure and composition. The freed electron is then accelerated towards the positively charged central wire, gaining energy and colliding with another gas atom. This atom is ionised as well, freeing a second electron. If the voltage on the central wire is high enough and the gas pressure is in a particular range, this process rapidly recurs until a charge 'avalanche', akin to a microscopic lightning strike, occurs between the centre wire and outer tube. Such an avalanche produces a discharge, which is then amplified electronically and converted into a measurable signal.

This type of counter signals when a highly energetic X- or gamma ray is detected, but gives no information about its energy. To measure energy, the counter needs to be operated at a somewhat lower voltage and possibly a different gas pressure. When these two parameters are adjusted correctly, the number of electrons created during subsequent ionisations after the initial collision of the gamma ray is *proportional* to the energy of the incoming gamma or X-ray photon. Hence the name *proportional counter*. A schematic diagram of such a proportional counter is shown in figure 1.5.

Because of their ability to count individual photons, and also retain information on the energy of the detected photon, proportional counters were rapidly adopted as the workhorse detector of X-ray astronomy in the 1960s and 1970s. However, their use for low-energy

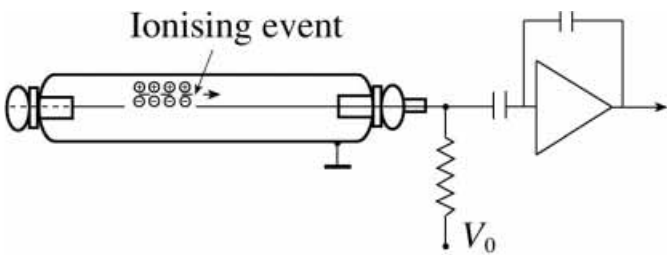

Fig. 1.5. Schematic diagram of a proportional counter (from Zombeck 1990).

X-rays (≈10–100 Å) or EUV (>100 Å) required some improvements. First, the window used in high-energy X-ray proportional counters would absorb all the lower energy X-rays or EUV radiation. So thinner windows were required that would allow these low-energy photons through and yet be strong enough to contain the counter gas. Certain plastics, such as polypropylene, were found to have these properties. Unfortunately, when made thin enough to be transparent to soft X-rays, most were found to be permeable to the gas molecules, causing a slow leak in the counter. Thus a gas flow system was needed to maintain the fill pressure and gas purity, resulting in the so-called 'thin-window, gas-flow' proportional counter.

For the very softest X-rays and EUV photons, extremely thin windows and low gas pressures are required. In an early search for EUV sources near the north galactic pole, astronomers at the University of California at Berkeley developed counters with polypropylene windows as thin as 0.3 μm. In addition, the gas itself had to be chosen to be less absorbing in the EUV region, so organic molecules such as methane (CH_3) or propane (C_3H_8) were used. These counters worked reasonably well, but operating them at wavelengths much longer than 200 Å was not possible due to limitations in window materials and gas properties. In addition, the unique feature of the proportional counter – its ability to measure photon energy – diminished, as the uncertainty in the measured photon energy was about the same as the photon energy itself in the EUV. Other approaches have proved to have a wider application for EUV astronomy: these were the channel electron multiplier (CEM) and later, the micro channelplate (MCP).

1.3.2 Photomultipliers and channel electron multipliers

Photomultiplier tubes have been used for decades to detect visible and ultraviolet photons at extremely low intensity levels. A photomultiplier tube is an evacuated glass tube with a light-sensitive surface (a photocathode): a photon striking the photocathode will eject an electron (with some probability – typically a few to 20%). After the photocathode is a series of plates which, when struck by the photoejected electron, emit additional (i.e. secondary) electrons. The plates are connected to a high-voltage supply through a series of resistors. Thus the electrons emitted from successive plates 'see' an electric field which accelerates them towards the next plate in the series. At the end of the series of plates, or stages, a single electron will have been amplified into a pulse of 10^7–10^{10} electrons, which in turn is collected by a metal plate and sensed through external electronics. Thus, just as in the Geiger counter, a single photon of visible or UV light may be detected using the photomultiplier.

The CEM is a compact, windowless version of the photomultiplier. Instead of a sealed tube, the CEM itself must be used in a high vacuum (about a billionth of atmospheric pressure). The photocathode of the CEM may be a cone covered with a photosensitive material (in the EUV this may be MgF_2, CsI or KBr) with a hole at its apex. Attached to the hole is a small-diameter tube (frequently a few millimetres or less) of lead glass coated with a material that acts much like the electron-emitting plates in a photomultiplier (see figure 1.6). The leading part of the inner wall of the tube may also act as the photocathode. The tube is often curved, and a high voltage is applied to one end. Just as in the photomultiplier, an electron ejected when a photon strikes the conical photcathode is accelerated towards the tube at the apex of the cone. When it strikes the tube's surface, secondary electrons are emitted, which in turn are accelerated further along the length of the tube, striking the tube wall within a short distance. The process will be repeated until, as in the case of the photomultiplier, a large pulse

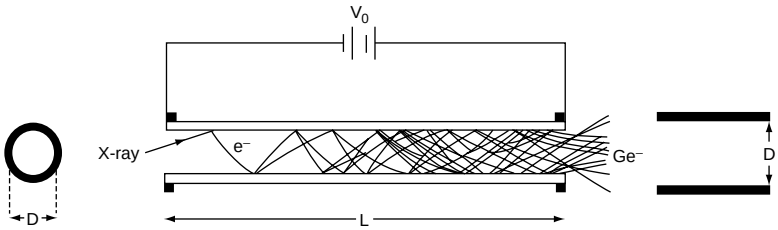

Fig. 1.6. Diagram illustrating the operation of a continuous-dynode electron multiplier (from Fraser 1989).

of about 10^6–10^7 electrons can be collected at the end of the tube and sensed electronically. The windowless nature of the CEM means that it may be used to detect photons at all EUV wavelengths.

1.4 Early experiments with sounding rockets

With the realisation that many galactic EUV sources could conceivably be detected from above the Earth's atmosphere, the Space Sciences Laboratory of the University of California (UC) at Berkeley embarked on a sounding rocket programme. Several experiments were flown between 1972 and 1974 to search for sources of EUV emission. These early experiments did not use imaging instruments, although nested gold-coated plane mirrors were employed as a flux concentrator. A mechanical collimator was used to constrain the field of view to $1^\circ \times 50^\circ$ full width half maximum (fwhm). The collecting area was divided into five overlapping segments each covered with a channel electron multiplier (CEM) photon detector.

A bandpass of 135–475 Å was defined using thin-film filters composed of aluminium and carbon. During the first flight of this instrument an area of sky approximately 1350 square degrees around the north galactic pole was surveyed, with a limiting sensitivity of 4.3×10^{-8} erg cm^{-2} s^{-1} (Henry *et al*. 1975). An improved second flight covered a similar area, achieving a flux limit of 2.9×10^{-8} ergs cm^{-2} s^{-1} (Henry *et al*. 1976a). No sources were detected on either flight. However, 3σ upper limits were obtained for the cataclysmic variables RX Andromedae, during flare, and U Geminorum, during quiescence.

Experiments were also carried out using five propane-filled proportional counters as detectors (Henry *et al*. 1976b). One disadvantage of these devices is the need for a gas-tight entrance window, restricting the useful wavelength range to the lower range of the EUV, where the absorption of the window is lowest. Although an additional wavelength-defining filter may then not be needed, counter windows usually need to be thicker than the thin-film filters employed with CEM experiments. Spanning a wavelength range 44–165 Å and with a field of view approximately $2^\circ \times 15^\circ$, some 3700 square degrees around the south celestial pole were surveyed, resulting in the detection of a single source with a flux of 1.3×10^{-9} ergs cm^{-2} s^{-1}. The most likely counterpart in the source error box was the cataclysmic variable VW Hydri.

Other investigators also carried out experiments with sounding rockets, including a group from California Institute of Technology. Using a spiraltron detector (a CEM coiled in a spiral) upper limits were obtained in the wavelength range 140–430 Å but no further sources were detected. The main limitations of all these sounding rocket payloads were the effective areas available with the existing technology, restrictions on payload dimensions and the short

exposures (300–500 s) allowed by sub-orbital flights. A chance to increase the exposure times with a longer duration space mission appeared with the Apollo–Soyuz Test Project.

1.5 EUV astronomy on the Apollo–Soyuz mission

In 1975, an opportunity arose to perform an extended search for EUV sources of cosmic radiation on the Soviet–American Apollo–Soyuz mission (officially termed the Apollo–Soyuz Test Project, or ASTP). In July of that year, US and Soviet astronauts were to link up in space in a demonstration of international good will. NASA realised that, in addition to the political benefits of the flight, some science instruments could 'piggyback' on the Apollo capsule, and solicited proposals for experiments which could be flown over the 9-day duration of the mission. The UC Berkeley group received approval for two such experiments: the Extreme Ultraviolet Telescope (EUVT) and the Interstellar Helium Glow Experiment. The results from the latter experiment, which was intended to map out the distribution and motion of He and He^+ in the heliosphere, were described in detail by Bowyer *et al*. (1977a). In the remainder of this section, we will concentrate on results from the EUVT, including the first unambiguous detection of a cosmic EUV source, the hot white dwarf HZ 43.

The EUVT (figure 1.7) was, in reality, not an imaging telescope at all, but a 'light bucket', consisting of four concentric Au-coated paraboloidal mirrors which focused EUV radiation onto one of two channel electron multiplier (CEM) detectors, one with a 2.5° diameter field of view (FOV) and the other with a 4.3° FOV (see Bowyer *et al*. 1977b). Just in front of the detector was a six-position filter wheel, with four EUV filters (parylene N, Be/Par N, Al + C, Sn), one far-UV filter (BaF_2) and a 'blank' position consisting of a thin Al disc for use in determining instrumental background. The sensitivity of the EUVT for the four EUV bands is given in figure 1.8.

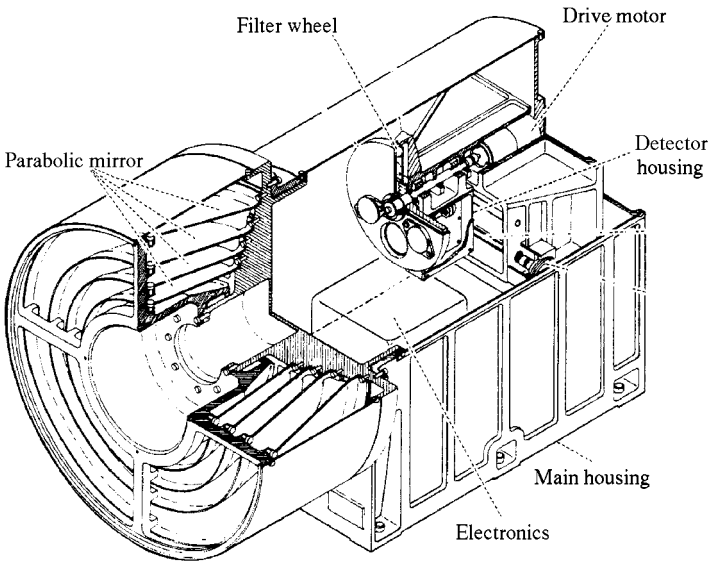

Fig. 1.7. A schematic diagram of the EUV telescope (EUVT) flown on board the Apollo–Soyuz mission in 1975 (courtesy S. Bowyer).

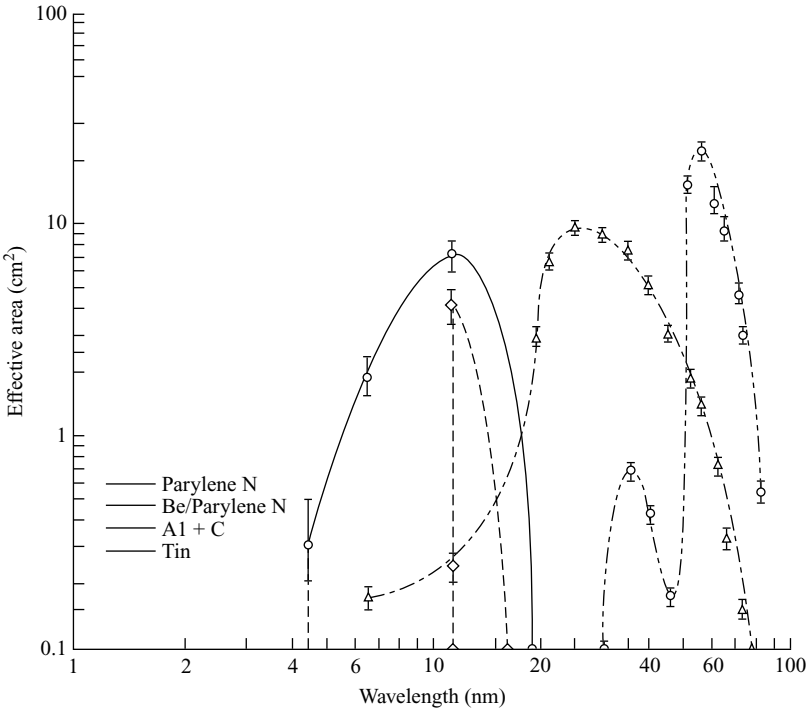

Fig. 1.8. Effective area of the EUV telescope (EUVT) on the Apollo–Soyuz Test Project (courtesy S. Bowyer).

The EUVT was mounted in the Service Module (SM) portion of the Apollo Command and Service Module (CSM), i.e. in the drum-shaped portion of the Apollo spacecraft behind the cone-shaped section which housed the Apollo crew. Operation of the EUVT was quite simple. Since the EUVT was rigidly fixed to the Apollo SM, the Apollo crew first had to orient the spacecraft such that the EUVT pointed at a given celestial target or background. Then an instrument door was opened, the EUVT turned on, one or the other of the two CEM detectors was selected, and the observing run begun. The filter wheel was designed to continuously step, so that all six positions would cycle in 6 s (10 rpm). The typical target observation sequence consisted of spending equal amounts of time pointing at a target and at two background points located on either side of the target, for total observing times of several to 20 min. More than 30 potential EUV sources were observed over about 15 Apollo orbits, some more than once. In addition, data from spacecraft slews in between targeted observations were included in a study of the EUV background, along with the background pointings from the targeted observations (Stern and Bowyer 1979).

It is worth noting that, at the time of the ASTP mission, there existed only educated guesses as to which stars would be both strong EUV emitters and would also have a low enough interstellar absorption so as to be detectable by the EUVT. Neither the first High Energy Astronomical Observatory (HEAO-1) nor the Einstein observatory X-ray missions had yet been launched, and, in fact, the first detection of a stellar corona (other than that of the Sun) associated with the binary system Capella (α Aurigae; Catura *et al*. 1975) had only just

occurred. In retrospect, the target list provided a good indication of which stars would also be later detected during the Roentgen Satellit (ROSAT) and Extreme Ultraviolet Explorer (EUVE) missions (see chapters 3 and 4). The target list consisted of:

- nearby stars with potential steady or flaring coronal emission: α Cen, ϵ Eri, 70 Oph, 61 Cyg, α Aql, *i* Boo, Proxima Centauri, Wolf 424, UV Cet, and β Hydri, EV Lac, θ Oph, α PsA,
- hot white dwarfs or central stars of planetary nebulae: HZ 43, HZ 29, Feige 24, BD $+ 28^{\circ}4211$, NGC 7293, NGC 6853,
- cataclysmic variable stars or dwarf novae: SS Cyg, AE Aqr, VW Cep, DQ Her, Z Cha, VW Hyi,
- nearby pulsars: PSR $1929 + 10$, PSR $1133 + 16$, PSR $1451 - 68$, and
- Jupiter(!)

The principal contribution of the EUVT on ASTP was the detection of four prototypical sources of EUV radiation: two hot white dwarfs, HZ 43 (Lampton *et al*. 1976a) and Feige 24 (Margon *et al.* 1976), a cataclysmic variable star (dwarf nova) SS Cyg (Margon *et al.* 1978), and the nearby flare star Proxima Centauri (Haisch *et al.* 1977). Only the two white dwarfs were detected as steady sources: in the original Lampton *et al.* (1976a) paper, the temperature of HZ 43's surface was estimated using a blackbody model to be $\sim 10^5$ K, although we now know, using a combination of optical and EUV spectroscopy, that the photospheric temperature of HZ 43 is closer to 50 000 K (see chapter 8). It is, however, still one of the hottest white dwarfs known, and remains to this day a 'standard candle' for all other EUV sources. Remarkably, HZ 43 is $\approx$65 pc distant, clearly demonstrating that the ISM was transparent enough, at least in some directions, to allow the observation of cosmic EUV sources. Subseqently, over 100 EUV emitting white dwarfs have been catalogued (Pounds *et al.* 1993; Bowyer *et al.* 1996), comprising the second largest population of EUV emitting objects. SS Cyg was caught in outburst in the shortest wavelength band of the EUVT: nearly 20 years later, the inexplicable spectrum of another dwarf nova caught in outburst, VW Hyi proved a challenge to theorists trying to understand the nature of the EUV emitting region (Mauche *et al.* 1996). Finally, the detection of Prox Cen during a flare was a harbinger of the hundreds of coronal sources seen by the ROSAT Wide Field Camera (WFC) and EUVE, not to mention the tens of thousands of stellar coronae detected in the ROSAT all-sky X-ray survey. Thus the ASTP mission demonstrated that EUV astronomy was feasible, that the 'unobservable ultraviolet' was a myth, and that future missions with greater sensitvity could begin to explore this wavelength region with some expectation of success.

1.6 After Apollo–Soyuz

Following the outstanding success of the EUVT on ASTP but without immediate prospect of a longer term space mission, further attempts at observations in the EUV were made with sounding rockets. Technological improvements led to the first true imaging EUV telescope flown by Berkeley. This payload made the first use of a focusing grazing incidence telescope. The use of grazing incidence telescopes in both X-ray and EUV astronomy gives a major improvement in sensitivity for two reasons. First, they can be used to increase the geometric area over which flux is collected without the need for very large detector areas. Second, being able to concentrate the image of a source in a small region of the detector yields a dramatic

improvement in signal to background ratio, as most of the unwanted counts lie outside the source image.

Several designs for focusing optics have been used. The most useful are the three designs originated by Wolter (1952a,b). Of these the Wolter Type III (figure 1.9) is too complex to

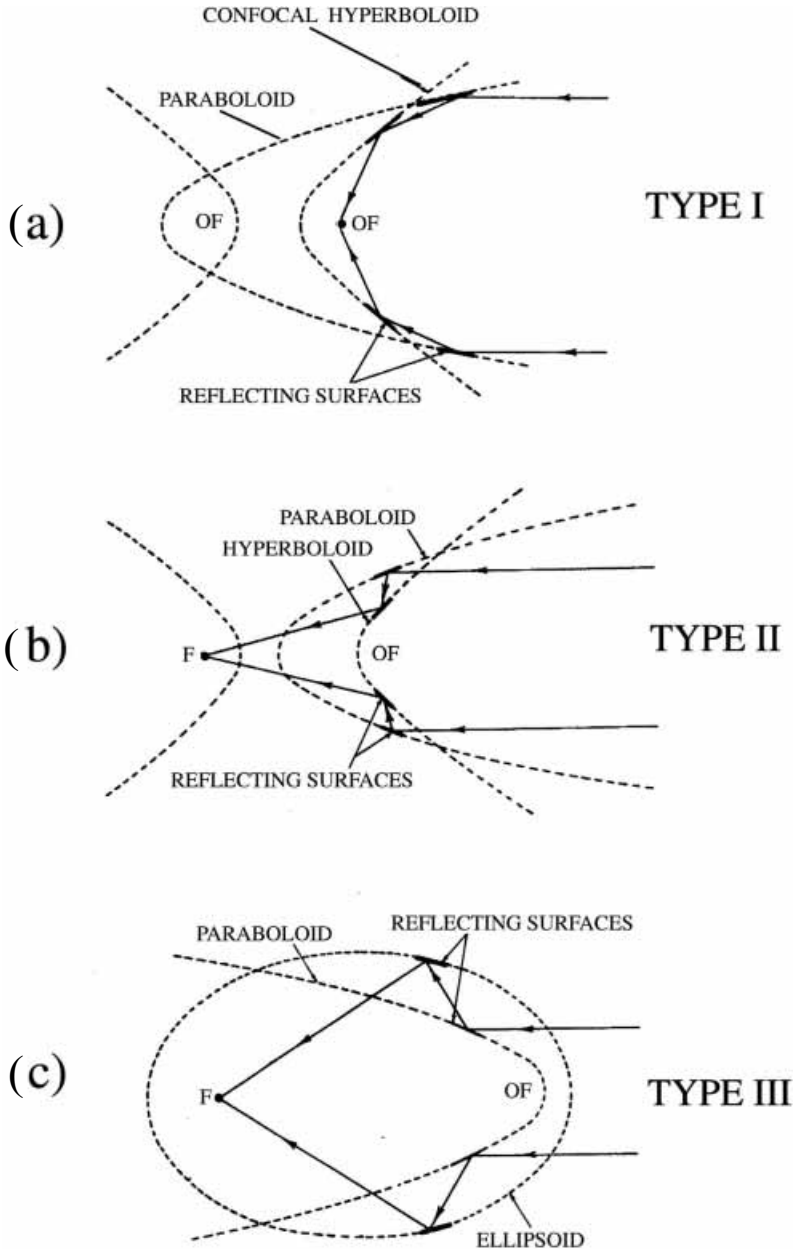

Fig. 1.9. The three configurations of X-ray (and EUV) imaging telescopes suggested by Wolter (1952a,b).

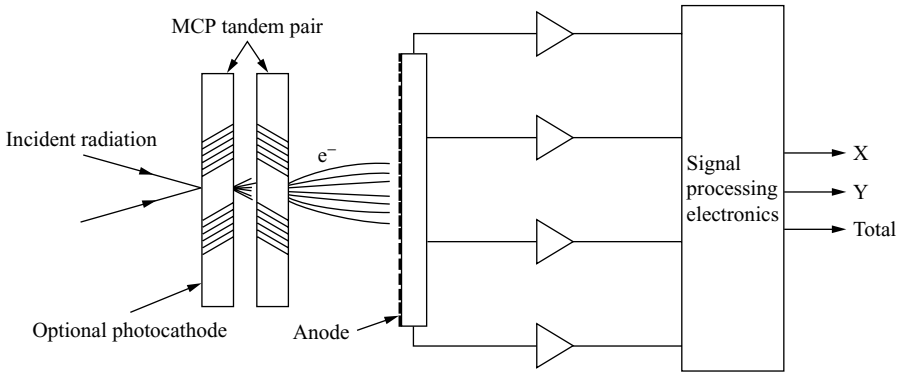

Fig. 1.10. Schematic diagram of an imaging microchannel plate detector.

be practical, besides having a small collecting area for a given telescope diameter, but both Type I and Type II optics have found application in EUV astronomy. The Type I is well-suited to wide-field survey applications since it suffers less from off-axis aberrations than the Type II. However, in the Type I the wide angle of the focused cone of light is difficult to use in a spectroscopic experiment and the Type II design has been preferred for such applications. Working at longer wavelengths than X-ray mirrors the tolerances on surface roughness are not so severe and, in the EUV, it has been possible to use lightweight mirrors, made from an aluminium substrate plated with nickel and overcoated with gold, to enhance the reflectivity.

To take advantage of the benefits of an imaging telescope requires a two-dimensional EUV detector. The main techniques used so far have been the microchannel-plate (MCP) detector and the imaging proportional counter. MCPs are arrays of single channel electron multipliers that have been miniaturised using technology similar to that used to manufacture optical fibres. Each plate comprises 10 million or more individual multipliers whose positions can be encoded by a range of output anode designs (e.g. figure 1.10). Alternatively, imaging proportional counters (IPCs or position sensitive proportional counters, PSPCs) can be used in the focal plane. Usually, arrays of wire grids are used to encode the positions in these devices (e.g. figure 2.11). However, as in the non-imaging versions, absorption of the incident EUV radiation by the counter window is a problem.

Berkeley's rocket-borne imaging telescope made use of a Wolter–Schwarzchild Type II mirror design (see section 2.3) and employed a MCP detector in the focal plane. EUV pass bands were determined by two filters with responses peaking at 300 Å and 500 Å. Despite the improved technical performance of the instrument only upper limits were obtained for the three white dwarfs observed – Sirius B (Cash *et al*. 1978), Feige 24 and G191–B2B (Cash *et al*. 1979). However, the factor of ten improvement over the limit obtained for Sirius B by ASTP is a good indication of the advantage of an imaging system.

A Dutch/Japanese collaboration developed a sounding rocket payload carrying two detection systems covering the band 50–270 Å. One of these was a one-dimensional X-ray focusing collector with PSPC detector while the second comprised eight large-area collimated proportional counters having a range of entrance windows (Bleeker *et al*. 1978). This payload obtained the first spectrum of an EUV source, the hot white dwarf HZ 43.

1.7 Sources of EUV sky background

1.7.1 Geocoronal background

So far, our discussion has concentrated on the development of EUV astronomy in the context of the detection of EUV sources. However, the EUV sky background plays a significant role in the process of source detection since the source flux must be sufficient to render the source visible above the background. There are two separate sources of background; the yet to be detected cosmic sky background, arising from hot gas in the ISM, and emission arising from the Earth's local environment. The cosmic background is potentially an interesting astrophysical source and it is therefore important to separate the two components. There are two contributions to the local background, the plasmasphere (geocoronal radiation) and the interplanetary medium, but the former is by far the largest component.

The Earth is surrounded by extensive clouds of hydrogen and helium, the geocorona, which result from the gradual loss of these gases from the Earth's atmosphere. The geocoronal background arises from resonant scattering of solar EUV radiation incident on these gases, which has an intensity of $\approx$1 erg cm^{-2} s^{-1}, mostly in the form of line radiation. The intensity of the scattered radiation will depend upon the number of atomic and ionic species present, the level of solar activity and the viewing geometry of the instrument. Below 1000 Å the lines of He I 584 Å and He II 304 Å predominate. Much weaker flux from He II 256 Å and He II 237 Å is also present. The general variation of these emissions with the solar zenith angle (the angle between Sun, Earth and satellite, see figure 1.11) and magnetic latitude was established in the mid 1970s by Meier and Weller (1974, He I) and Weller and Meier (1974, He II). In both cases, minimum intensity occurs when the satellite is at its nadir with respect to the Sun and when the view direction is along the Earth shadow. Maximum He I flux ($\approx$50 Rayleighs, 1 R $= 7.96 \times 10^4$ photons cm^{-2} s^{-1} sr^{-1}) occurs during the daytime (solar zenith angle $<90^\circ$) and appears to be independent of the view direction. At night the flux

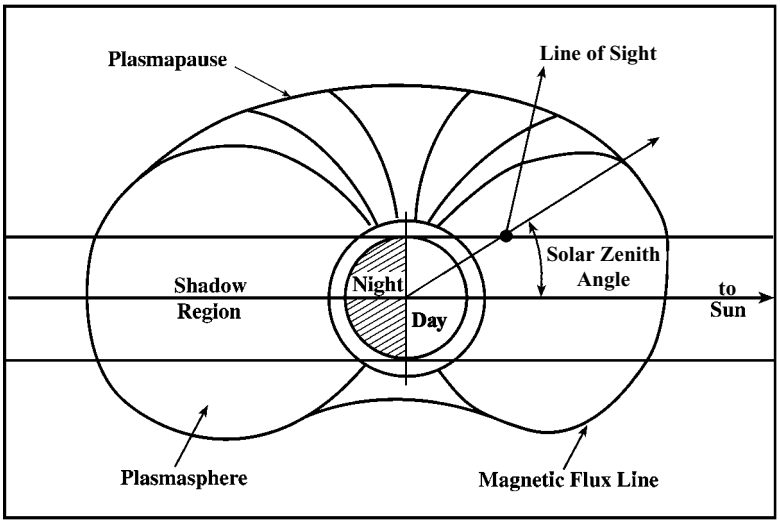

Fig. 1.11. Observing geometry for a spacecraft in low Earth orbit, defining the solar zenith angle and illustrating the region of the Earth shadow.

drops by two orders of magnitude or more to a minimum, looking along the Earth shadow. This night-time flux is the contribution from interplanetary helium (1–9 R, Weller 1981). Emission of He II (5 R maximum) is an order of magnitude below the He I flux, although it shows similar variation, but with some differences arising from the interaction between the ions and the Earth's magnetic field. The minimum contribution of He I in the Earth shadow is 0.03–1 R.

Above 1000 Å, the geocoronal spectrum is dominated by the emission lines of neutral hydrogen (1216 Å and 1025 Å) and those of neutral oxygen (1304 Å and 1356 Å). Although these lines lie outside the EUV, they are very bright and can still potentially contaminate EUV data if they 'leak' through any blocking filters. The lines of neutral hydrogen have been observed by satellite and sounding rocket experiments (Meier and Mange 1970; Young *et al*. 1971; Paresce *et al*. 1972; Thomas and Anderson 1976). At high altitude ($\approx$650 km), the intensity of Lyman α (1216 Å) radiation varies between about 10^3 and 2×10^4 R according to the solar zenith angle (Meier and Mange 1970; Thomas and Anderson 1976). Lines of OI may have similar intensity (Meier and Prinz 1971). These fluxes are considerably more intense than either of the strong He lines and must be efficiently rejected from any EUV instrumentation, by use of detectors that are blind to these far-UV wavelengths or suitable blocking filters.

1.7.2 The cosmic EUV background

EUV emission from hot gas is not necessarily confined to that from discrete stellar coronal sources or hot white dwarfs. Supernovae are expected to provide a source of hot gas in the ISM. Hence, apart from its absorbing effects on the emission from distant objects, it seems likely that the ISM may well be an EUV source in its own right, but a diffuse one, covering large areas of the sky. Real evidence for the existence of hot material, with temperature $\approx 10^6$ K, is provided by the diffuse soft X-ray background (deKorte *et al*. 1976; Sanders *et al*. 1977; Marshall 1982; Snowden *et al*. 1995). These results also indicate that the emission is local. The brightness distributions are patchy, unlike the isotropic and predominantly extragalactic higher energy background ($>$1 keV), and the correlation with the neutral hydrogen column density is not consistent with that expected from simple photoabsorption of the galactic flux. In addition, a number of energy-dependent large-scale features, such as the North Polar Spur, are discernible. The presence of OVI absorption lines in the spectra of hot stars also provides evidence for material with temperatures in excess of 10^5 K (e.g. Jenkins 1978).

Few direct measurements of any diffuse cosmic emission component were made in the early EUV astronomy experiments, mainly due to the difficulty of separating out the often overwhelming geocoronal component. Hence, predictions of the expected flux relied heavily on theoretical models. For example, Grewing (1975) derived a blackbody model ($T \approx 1.1 \times 10^4$ K) of the background between 1750 Å and 504 Å, showing that the flux is the result of contributions from a large number of O and B stars. The Apollo–Soyuz experiment was able to carry out an extensive survey of the EUV background in the 50–775 Å range (Stern and Bowyer 1979). At the longer wavelengths, the cosmic background was indeed masked by the geocoronal flux but an intense background was apparently observed in the 110–160 Å band, at a level of $\approx$4 photons cm^{-2} s^{-1} sr^{-1} Å^{-1}. A subsequent analysis (Stern and Bowyer 1980) concluded that, barring the existence of an unreasonable number density of EUV sources, the uniformity of the observed flux indicated that the emission was produced by a diffuse source.